Transportation Institute

Memo

To: T. Ahlborn, D. Harris, L. Sutter, R. Shuchman, and rest of Project Team

From: H. de Melo e Silva, C. Brooks, D. Banach, J. Burns, D. Dean, R. Dobson, A. Endsley, R. Hoensheid, R. Oats, K. Vaghefi

CC: C. Singh

Date: January 13, 2012

Number: 24

Subject: Project Progress Update Relating Technologies and Decision Support System to Health Indicators for Bridge Condition Assessment.

3D OPTICAL BRIDGE-EVALUATION SYSTEM (3DOBS)

The 3DOBS, a demonstration of 3D optics technology that uses close range photogrammetric principles, was successfully deployed to all field demonstration bridges to collect 3D bridge surface, as previously described in technical memorandum nº 21. The remote sensing team has focused on extending the maximum value from this successful demonstration of a practical, low cost remote sensing system that can characterize bridge deck surfaces with high-resolution elevation data.

An example of extending the value of the high-resolution Digital Elevation Model (DEM) data being generated for each bridge out of the 3DOBS is calculating the International Roughness Index (IRI) for all the field demonstration bridges. The IRI data is being incorporated into this project to help assess the overall health conditions of the pavement for the three tested bridges, which can be used as a component of the overall bridge health signature. The IRI profiling index has ratings ranging from 0 m/km (or mm/m) to 20 m/km; indicating a perfectly smooth surface and an extremely rough unpaved surface, respectively. The ratings are based on a longitudinal profile of the pavement, which is then processed through the quarter-car and 250 mm wavelength models to simulate how a single wheel of a vehicle would react to the condition of a pavement.

Normally the longitudinal profile is created from a series of measurements made by an altimeter connected to a car, which is driven across the pavement. However, for the purposes of this project, the elevation measurements were collected using a remote sensing methodology to determine where the three bridges would be positioned on the IRI graph (Figure 1) and to validate if the results were similar to their real-world conditions.

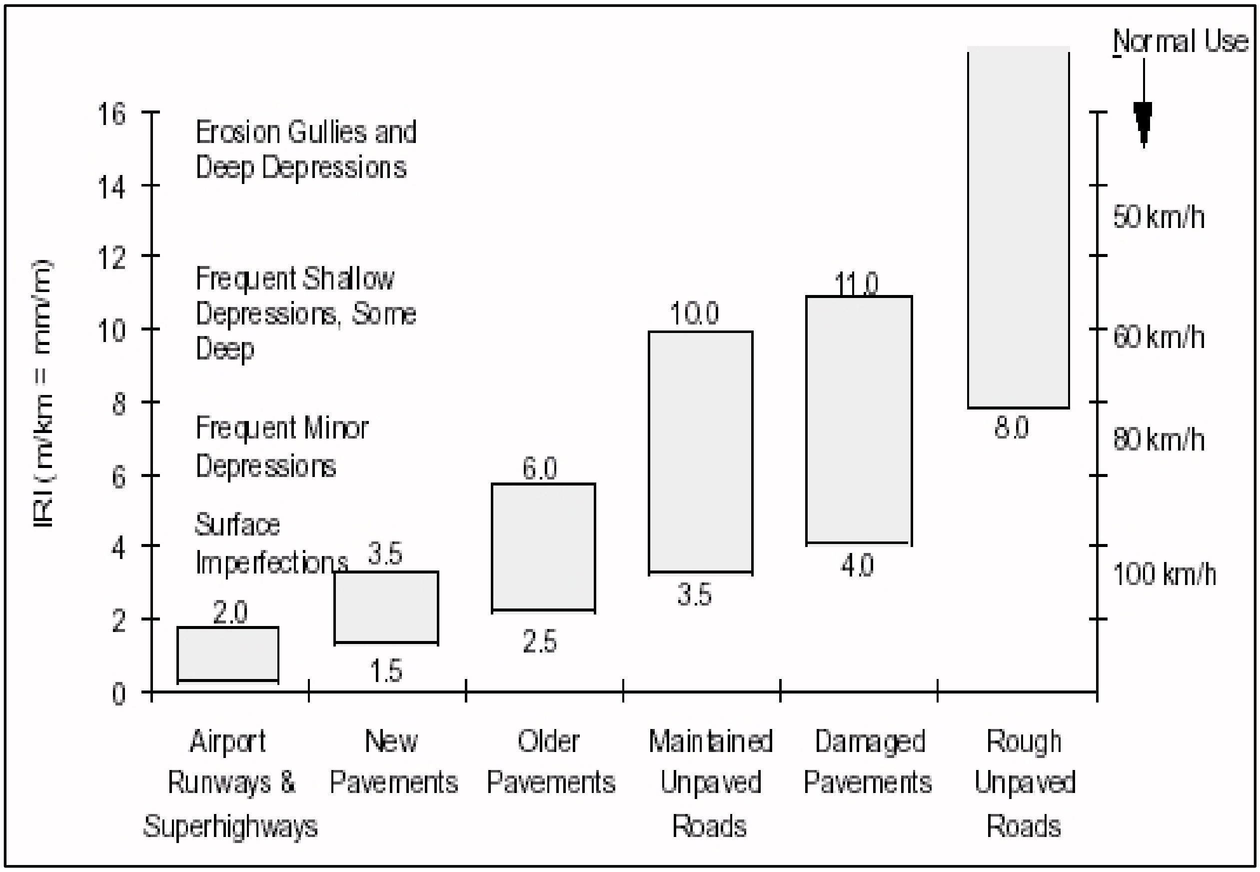

Figure 1: The International Roughness Index graph.

Collecting the pavement's elevation changes on the Freer Road bridge involved using a DEM created using the 3DOBS. This process contained the necessary data to create a zero plane, in which all elevation deviations were based on. The profiling data was then formatted into an Engineering Research Division (ERD) file format that was imported into a computer program, The Transtec Group ProVAL, used to view and analyze pavement profiles. ProVAL then graphed the longitudinal profile, which was processed through the two models. The end result is an IRI value that is indicative of a single wheel path across the bridge.

Figures 2 and 3 demonstrate the longitudinal profiles of two tire tracks for each side of the Freer Road bridge. The bridge deck-joints elevation data were removed from the profiles because they would misrepresent depressions on the bridge. After being processed through the two models, the northbound left tire track data produced an IRI value of 3.59 m/km, while the northbound right tire track data had an IRI value of 4.26 m/km. In addition, the southbound left tire track produced an IRI value of 4.14 m/km, and the southbound right tire track had an IRI value of 3.71 m/km (see Table 1). All of these roughness values were classified as “older pavements” according to the IRI graph. To validate the results, they were compared against what was known about the bridge. Similar to the IRI graph, the Freer Road bridge has an older pavement, has frequent minor depressions, and is a paved surface.

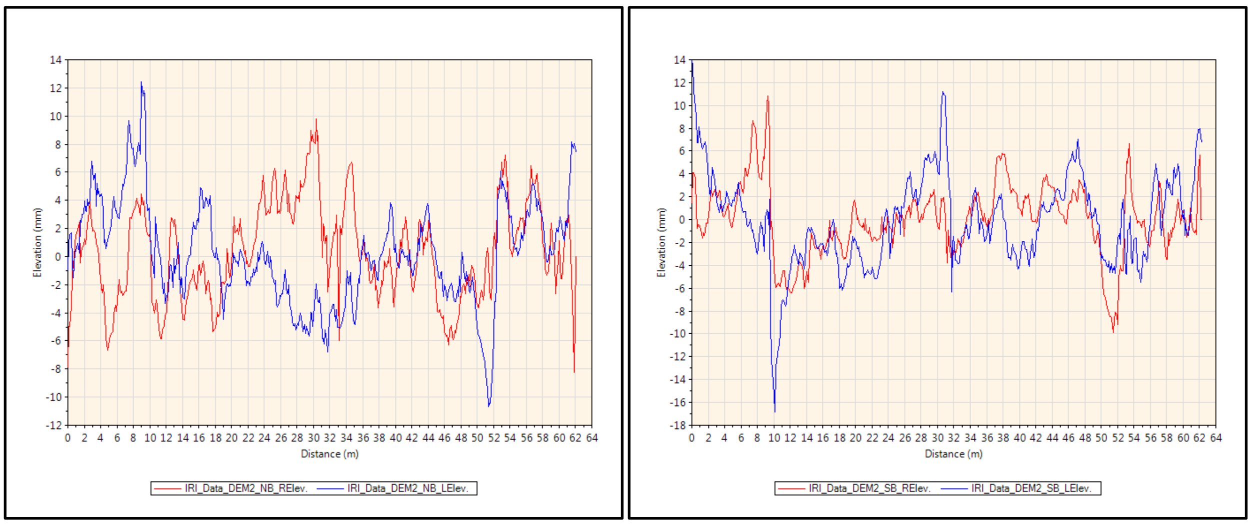

Figures 2 & 3: The longitudinal profiles of the bridge at Freer Road. Each indicates two tire tracks on the northbound (left) and southbound (right) lanes.

File	Profile	IRI (m/km)
IRI_Data_DEM2_NB	LElev.	3.59
IRI_Data_DEM2_NB	RElev.	4.26
IRI_Data_DEM2_SB	LElev.	4.14
IRI_Data_DEM2_SB	RElev.	3.71

Table 1: IRI values for each tire track on Freer Road.

In addition to this new IRI data analysis, the project team has continued to use the 3DOBS-derived bridge deck elevation data for detecting a variety of bridge condition indicators. The team has been able to determine the percent spalled of a bridge deck, location, area and volume of individual spalls, total area, and volume spalled. All of these are derived from a DEM that was generated from a single, inexpensive, rapidly-deployable vehicle mounted system.

An algorithm was created for the 3DOBS to automatically detect spalls from the DEM and calculates area and volume using focal statistics. This enabled rapid calculation of useful data to integrate into the Decision Support System (DSS) and has been labeled the "MTRI (Michigan Tech Research Institute) 3DOBS spall detection algorithm". One feature of the algorithm is that users can specify the minimum size of spall that they are interested in. With the use of the high resolution DEM produced by the 3DOBS (as detailed in technical memorandum nº 21), the remote sensing team is able to manually find spalls that are less than 10 cm^2 (1.55 in^2, or a circle having ∅1.41 in). However, at such a small size, there are artifacts in the DEM around a similar size. Theses artifacts would be difficult for an automated algorithm to differentiate from "real spalls" and therefore possibly produce incorrect results.

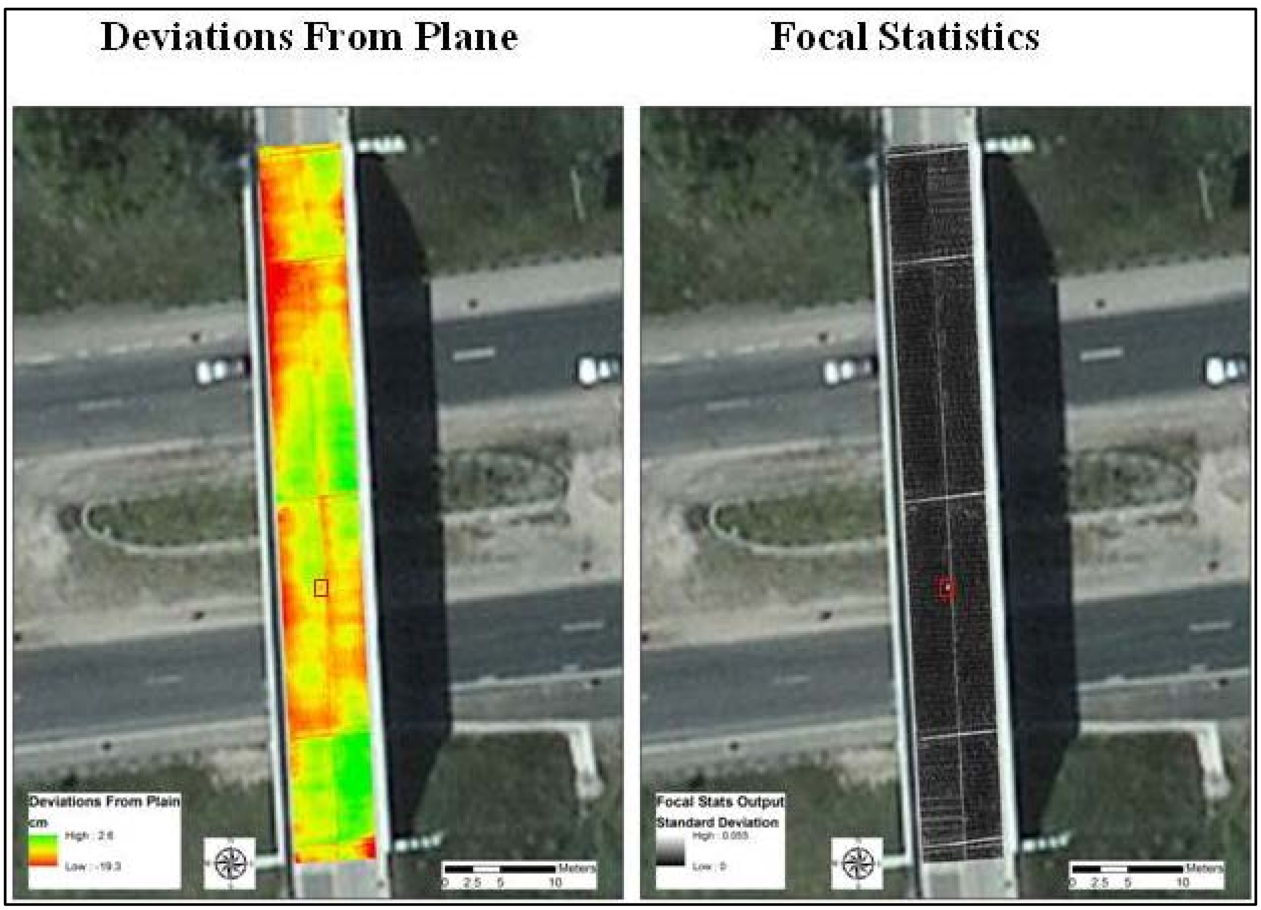

Figure 4: Comparison of the DEM and Focal Statistics output for the Freer Rd bridge.

The 3DOBS spall detection algorithm uses the focal statistics function found in Esri ArcGIS to locate spalls. This function determines the change in cell values as it relates to a specified “neighborhood” of cells. Figure 4 shows an example of the focal statistics output as it relates to the DEM. The red box on both the DEM and the focal statistics output shows the location of a rather large spall on the Freer Road bridge. This spall has a size of 11,429 cm^2 (12.3 ft^2). Figures 5 shows examples of the different sizes of the neighborhood that could be set within the focal statistics function. The top two are examples of a rectangular neighborhood and the bottom two are examples of a circular neighborhood with a specified radius of cells.

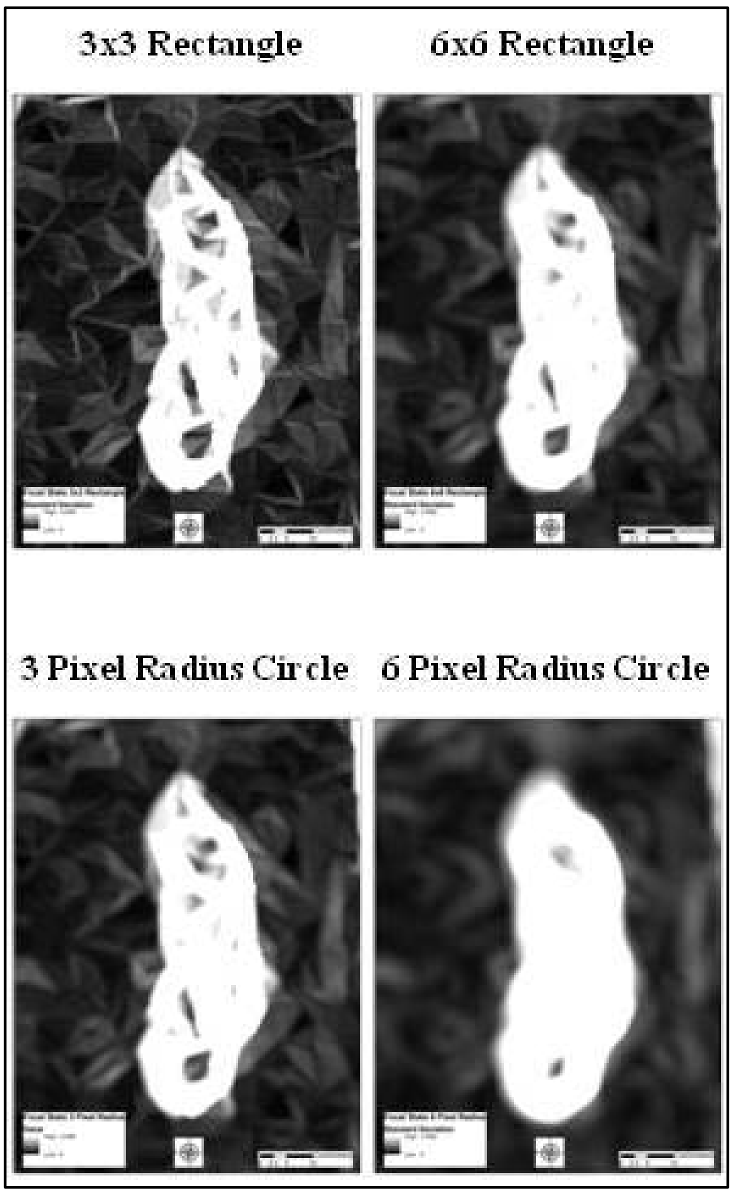

Figure 5: Comparison of the different "neighborhood" sizes and type that can be calculated.

Since the 3DOBS-derived elevation data can detect spalls at various minimum sizes, testing was done to see at what minimum size was optimal for accurately detecting spalls. Figure 6 shows an example of three different minimum sizes that were used. These minimum sizes were 10 cm^2, 100 cm^2 and 1,000 cm^2. From this testing, we determined that a minimum detection size of about 40 cm^2 (6.2 in^2) would be optimal.

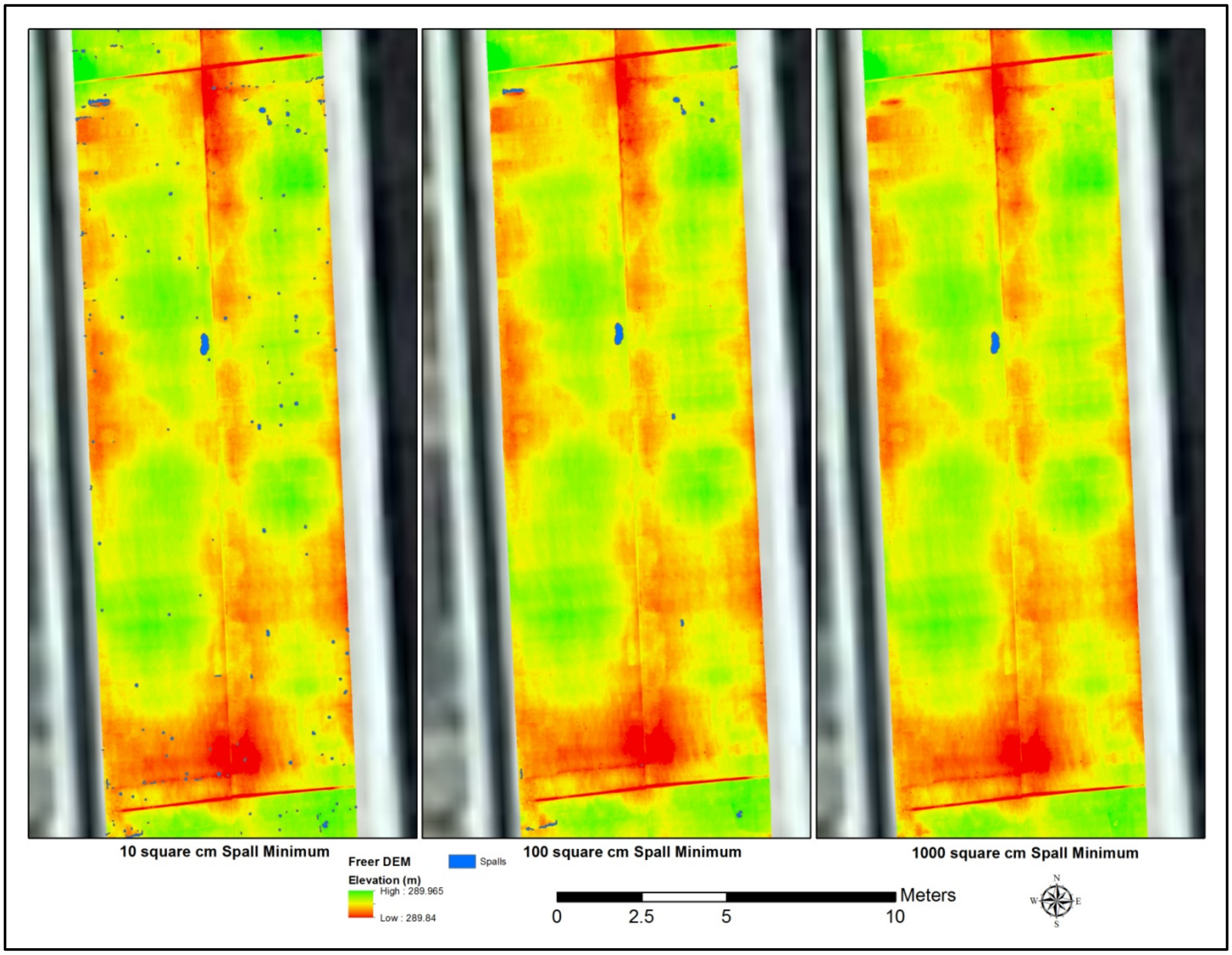

Figure 6: Comparison of three different minimum spall output sizes from the 3DOBS spall detection algorithm.

Table 2 is an example of the detailed output from the spall detection algorithm. This example is from the Freer Road bridge over I-94. The minimum spall size set for the algorithm is 40 cm^2, which is at a sufficient size to remove the artifacts. There were a total of 267 spalls detected with a total area of 48,141 cm^2 and a total volume of 80,700 cm^3. This means that Freer Road bridge is 0.85% spalled.

Another bridge that was visited was the Willow Road bridge over US-23 was somewhat different from the Freer Road bridge. There was a significant amount of spalling that was outside but adjacent to the driving area. Due to the field of view of the camera used for the 3DOBS, this area was represented in the DEM and subsequently in the algorithm analysis. If the total bridge is included in the calculation then the total spalled area is 369,814 cm^2 and volume is 1,980,300 cm^3 and the bridge would be 6.99% spalled. If, however, only the driving area of the bridge is then the total spalled area is 21,838 cm^2 and volume is 20,600 cm^3. The percent spalled drops to just 0.41% which is less than the Freer Road bridge.

ID	GRIDCODE	ORIG_FID	AREA	MAX	MIN	SP_VOLUME	SP_AREA
92	2	91	11883.75	289.96	289.84	0.0485	1.1429
983	2	982	5130.50	289.94	289.91	0.0079	0.5206
991	2	990	21092.50	289.95	289.91	0.0079	0.5282
1008	2	1007	1967.75	289.94	289.92	0.0028	0.1923
989	2	988	1840.75	289.94	289.91	0.0016	0.1796
1009	2	1008	1279.00	289.93	289.91	0.0013	0.1232
47	2	46	965.25	289.95	289.92	0.0012	0.1100
616	2	615	1208.75	289.94	289.91	0.0012	0.1264
942	2	941	872.50	289.95	289.94	0.0007	0.0873
75	2	74	2173.75	289.93	289.90	0.0007	0.0710
519	2	518	549.50	289.95	289.93	0.0005	0.0550
288	2	287	350.00	289.93	289.92	0.0003	0.0350
46	2	45	404.25	289.95	289.93	0.0002	0.0404
987	2	986	263.25	289.94	289.92	0.0002	0.0258
527	2	526	234.75	289.95	289.93	0.0002	0.0240
536	2	535	185.50	289.95	289.94	0.0002	0.0440
11	2	10	407.00	289.93	289.91	0.0002	0.0403
184	2	183	168.00	289.94	289.93	0.0001	0.0168
290	2	289	95.25	289.94	289.92	0.0001	0.0095
682	2	681	88.00	289.95	289.93	0.0001	0.0086

Table 2: Example output from the 3DOBS spall detection algorithm. The columns labeled "SP_VOLUME" and "SP_AREA" are the calculated volume and area measurements in m^3 and m^2.

Next Steps

During the next quarter of this project, the team's new ability to derive IRI data will be applied to the Willow Road bridge and both of the Mannsiding Road bridges. Each will have a digital elevation model built for them using the 3DOBS, upon which elevation data can be extracted. The end result will be IRI values for each of the bridges that should not only match the description given on the IRI graph but also be indicative of the deck surface condition health. The team will also complete the derivation of the 3DOBS DEM for the Mannsiding Road bridges, now that Freer and Willow Roads bridges are complete.

Technical memorandum nº 21 described the primary benefits of the 3DOBS as: low cost to purchase components, rapid deployment, limited time needed to collect data on the bridge, and that the team has demonstrated how to derive useful metrics of bridge deck condition. The ability to extract out additional useful metrics such as IRI can now be added.

The project team anticipates that transportation agencies will find additional uses for a very high resolution deck surface elevation data set that can be created rapidly and inexpensively.

BRIDGE VIEWER REMOTE CAMERA SYSTEM (BVRCS)

Additional work with the BVRCS was not needed during the past quarter. It continues to be an inexpensive, easily deployable way of collecting location-tagged photo inventories of a bridge and its environs, deployable at any time a transportation agency would like to do so. The current level of technology could be deployed by a local or state transportation agency, and fully commercial system could easily be derived from this project's version. As a practical demonstration of Google Street View-style photography technology, further development is not anticipated in this project. The project team is now at the point that the photo inventory is being integrated into the DSS as a demonstration of how the photos could be used to visually assess current conditions and to future photo inventories as they become available.

GIGAPAN SYSTEM (GigaPan)

Similarly, the project team did not consider additional development of the GigaPan System necessary during the past quarter. Instead, the DSS part of the team has started to integrate the high-resolution photo inventory into the DSS so that transportation agencies can more easily understand how they can use this bridge photo inventory method. GigaPan continues to serve as a demonstration of a relatively inexpensive hardware that creates a high-resolution photo inventory of parts of a bridge, available as a single gigapixel image stitched together from hundreds or thousands of digital photos, with the limitation of the time needed to process the images into a single photo, as described in technical memorandum nº 21.

THERMAL INFRARED (ThIR)

In this quarter, preliminary ThIR results for the Freer Road bridge were compared with the Michigan Department of Transportation (MDOT) hammer sounding technique. In this method, a photo of the whole bridge was created and imported into ArcGIS to show the boundaries of delaminations that were marked by bridge inspectors on site (see Figure 26). By creating a layer for these areas, the total area of delamination can be calculated in ArcGIS. The total "hammer sounding" area calculated was 101 ft^2 compared to 29 ft^2 using the ThIR method (corrected from 22.95 ft^2, see technical memorandum nº 21). The difference is mainly because of the limitation for identifying the exact boundaries of each delamination by inspectors on site and/or not having good quality images for some areas.

There were two main problems for this bridge; (1) delaminations around the construction joints on the center of the bridge and (2) the painted centerline stripe overlapping delaminated areas. Because the ThIR camera works with reflective energy, the paint affects readings, having at times an adverse effect on the interpretation of the images in this area. Figure 7 shows delaminations around centerline area and Figure 8 shows the difference between boundaries of MDOT marked area and ThIR images.

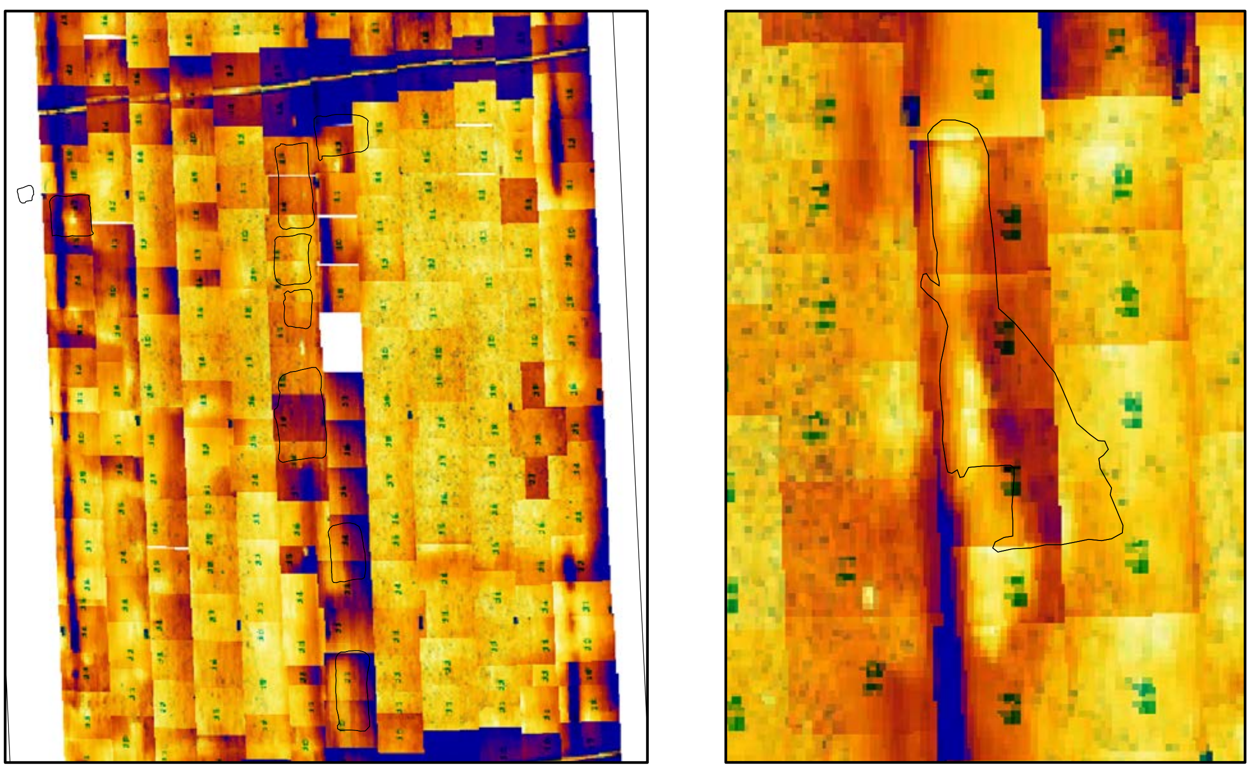

Figures 7 & 8: MDOT delamination map and ThIR image superimposed on each other.

The ThIR data for the Willow Road bridge has been analyzed with the same method that was discussed in technical memorandum nº 21 for the Freer Road bridge. Shoulders of this bridge were in bad condition at the time of inspection, therefore the total area of delamination was calculated without considering the images taken from the shoulders. Table 3 summarizes the results of this calculation.

Total Delaminated Area (ft^2)	140.95
Total Bridge Area (ft^2)	5,015.75
Percentage of delamination (%)	2.81

Table 3: Willow Road bridge ThIR preliminary results.

Figure 9 shows the ThIR image(s) of the Willow Road bridge and Figure 10 shows the MDOT-marked areas of delamination which were imported into the ArcGIS environment (see Figure 26). The total area of delamination based on one of MDOT's current practices (hammer sound) was calculated to be 159.54 ft^2 using ArcGIS. This indicates that 3.18% of the bridge deck is delaminated. Based on the ThIR images the delaminated area of the bridge deck was calculated to be 141 ft^2. This corresponds to 2.81% of the bridge deck being delaminated. Note that the spray-painted areas marking the delamitations are possibly 'over marked'.

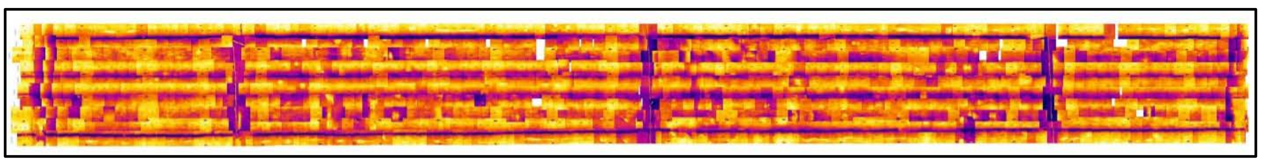

Figure 9: Willow Road bridge ThIR image.

Figure 10: Willow Road bridge MDOT hammer sounding delamination survey.

Next Steps

Next quarter of this project will be focused on extracting delamination information from ThIR images for Mannsiding Road bridges and summarizing the results based on percent delamination that can be imported and displayed in the DSS to help bridge inspectors. In parallel the project team is still developing a The MathWorks MATLAB algorithm to process large amounts of data, automatically stitch the photos, and calculate the area of delamination. Limitations of applying this technology on a bridge has been discussed in technical memorandum nº 21 and investigations are under consideration to overcome those barriers and improve data collection methods and results.

DIGITAL IMAGE CORRELATION (DIC)

As discussed previously in technical memorandum nº 21, DIC was implemented during field demonstrations and revealed to have many benefits and limitations. Additionally, the limitations initiated more investigation of this method's processing algorithms and a more stable data collection system. The overall goal of additional investigation will allow for improvements on analysis of bridge health indicators at the global behavior level.

In previous tests, the 318.25 MTS 810 Material Test System was used for DIC measurements. This testing machine was implemented again to monitor movement with a PCB Piezotronics 333B50 piezoelectric accelerometer and transform (integrate) those readings into displacement. Measuring this data can enable a measurement of environmental noise (i.e., vibration or movement on the camera) that can be factored out to capture the true bridge movement measurement (see Figure 11).

In the previous set of tests as reported in technical memorandum nº 21, there was substantial noise encountered in the set due to environmental conditions. Using the MTS system, a known displacement measurement can be used and therefore an easier integration into displacement measurements can be obtained. The accelerometers were connected to a Campbell Scientific CR9000X measurement and control system in which results were collected, filtered through, and presented graphically. The results of this test showed us that this method can allow for movement tracking using accelerometer data and integrating into position (displaced movement) measurements. A sample of this acceleration data plot is shown in Figure 12. These plots show the data from the raw accelerometer measurements and the expected displacement measurements determined using a MATLAB algorithm. In Figure 13, the calculated displacement plot of the test data is shown with units of meters and seconds. The measured displacement graph reveals the sinusoidal wave that was expected as the MTS system testing platform was moved in a cyclic motion for measurement comparisons. More investigation is being done to ensure the output data is correctly producing what is expected from the inputs. In this investigation, correct filtering procedures are evaluated as well as appropriate unit conversion. Both measurements are plotted versus the time.

Figure 11: Accelerometers on MTS testing machine.

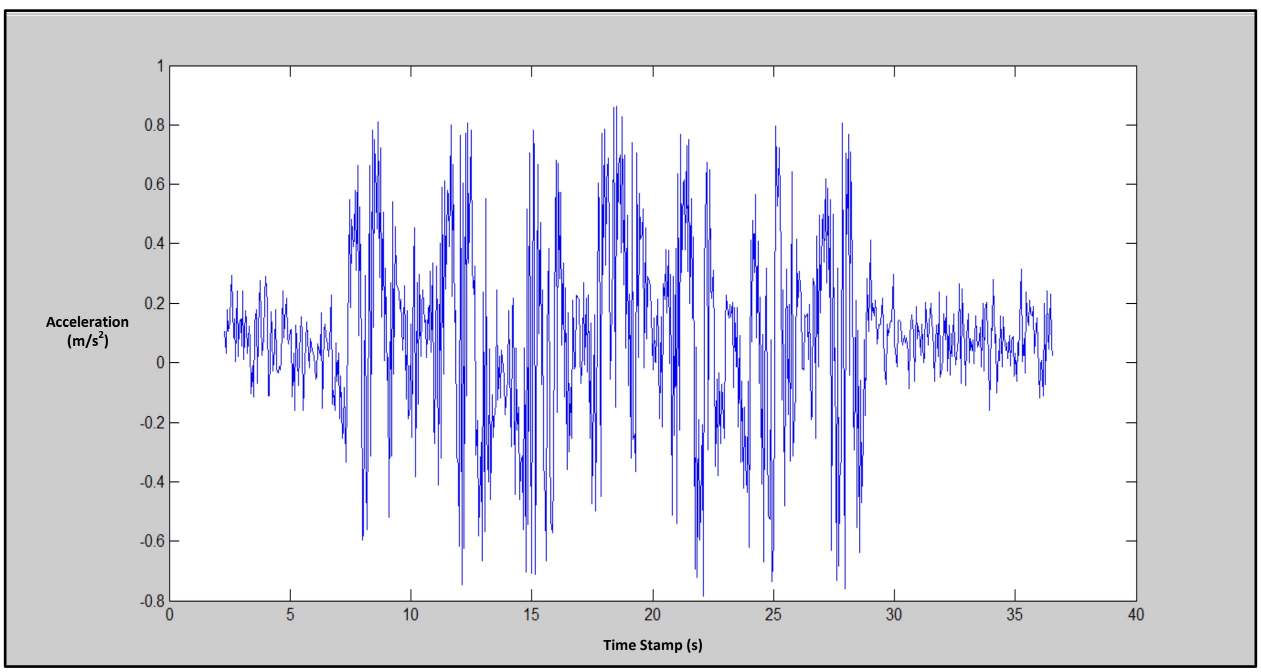

Figure 12: Plots of Acceleration and calculated displacement measurements.

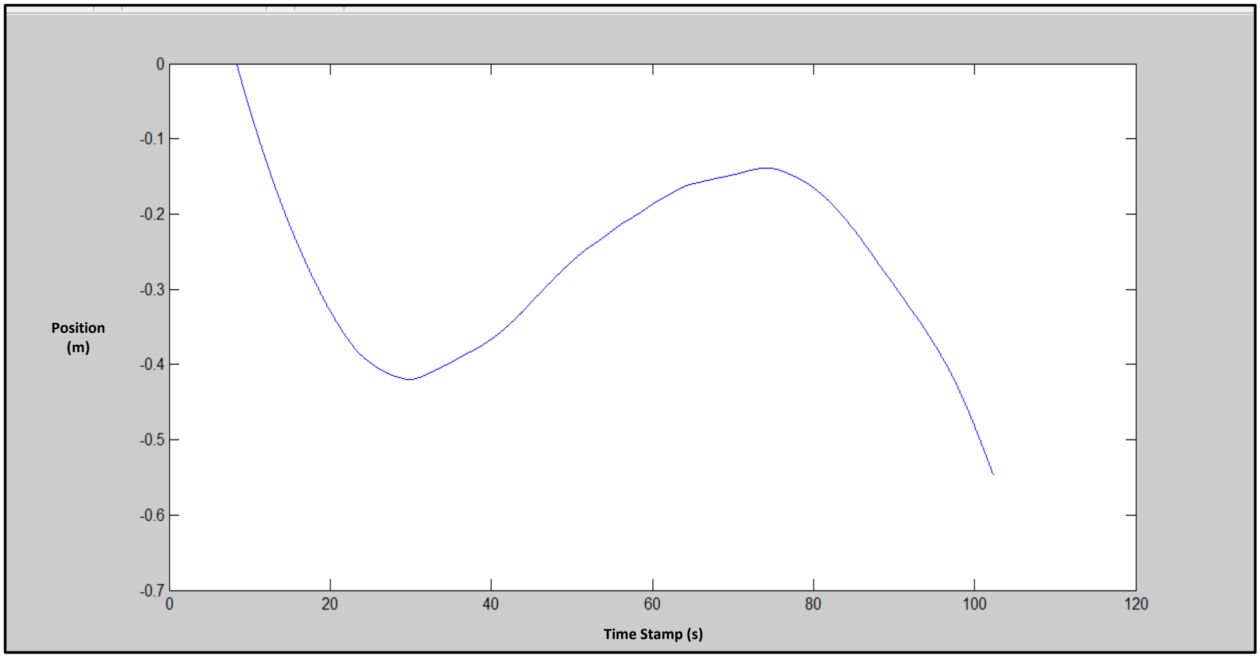

Figure 13: Plots of Acceleration and calculated displacement measurements.

As the generic method for capturing motion into displacement measurements on the MTS system, this was further configured for the camera-lens system. The camera-lens system (as used in DIC system) was connected with an accelerometer in order to measure the excessive movement endured and computed the movement as displacement. In this setup, a more stable and heavier surveying tripod as well as a wooden base ensuring a flat secure platform for the camera–lens system was employed. An additional accelerometer was also placed at the bottom of the tripod for location comparisons at the top and bottom of the tripod. These figures of the tripod and camera-lens setup can be shown in Figures 14 and 15.

The measurement of the camera movement(s) have shown similar results as in the testing system's data, but there were more unknown factors to consider in the acceleration measurement. The calculated position (displacement) measurement for this scenario reveals some alteration in what is expected and other parameters may have to be recognized in the setup and even in considering algorithms such as the input of the constant "c" values from the integration of the acceleration of the data (i.e., $\int$(acceleration) = velocity + "c" and similar in the integration of velocity for position) . This method allows for noise to be captured in measurements, but also may require an additional program to account for noise and other parameters associated with system inputs and obtaining correct bridge structure movement.

Moreover, stabilizing systems are being considered and should be implemented in the future. As an example, a gyroscopically-compensated camera mount, such as one of the Kenyon

Laboratories (<http://www.ken-lab.com/>), could help in keeping the camera stable and minimized movement within the camera-lens system. Reduction of the standoff distance would certainly reduce the effects of excessive wind and vibration on the camera-lens system.

Figures 14 & 15: Camera on stable tripod and detailed of mounted accelerometer.

Next Steps

The benefits of the DIC system definitely show great promise for bridge health indicators, but alterations in data collection procedures and in the analysis algorithms can improve the measurements. As mentioned, DIC is beneficial in allowing flexibility in testing location and use of available software analysis. However, the software analysis is dependent on the inputs of the testing system and calibration of the testing environment (in which noise will have to be considered). For the DIC method, a more integral algorithm is being investigated that would accurately tracked the movement using optical images that also will consider noise movement as previously mentioned. Depending on the software used for analysis whether it is commercial (Correlated Solutions Vic-2D) or not (MATLAB), more adjustments should be considered for accurate displacement measurements bearing in mind noise issues.

For future bridge comparison, a walking bridge (Figure 16) located in the Michigan Technological University (MTU) Benedict laboratory would provide a great case for implementation for testing alterations and variations of the DIC system and developed algorithms. In addition, equipment instrumentation on the walking bridge would be complemented in the future test scheme.

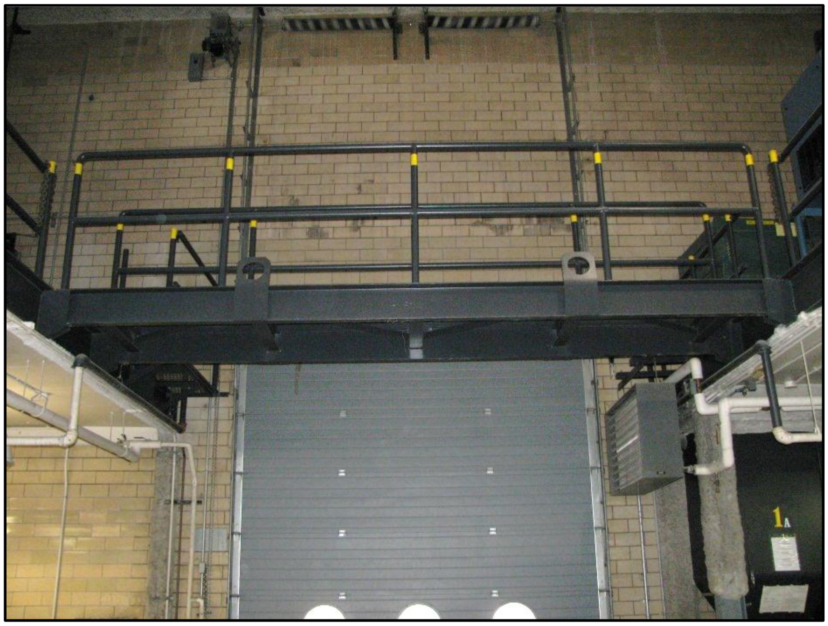

Figure 16: Walking bridge located in Benedict laboratory at MTU.

LIGHT DETECTING AND RANGING (LiDAR)

The remote sensing team has been focusing on extracting out useful bridge condition metrics out of the LiDAR scans of the study areas that were performed by an MDOT LiDAR crew (Kelvin Wixtrom and Shawn Roy) during the field campaigns in August, 2011 at Freer Road, Willow Road, and Mannsiding Road bridges (see Figure 17). Twenty scanner setups were performed at the Freer Road site, 18 setups were performed at Willow Road, and 12 setups each were performed for Mannsiding Road over northbound and southbound lanes of US-127. LiDAR scans were post processed by MDOT.

Certainty 3D TopoDOT, Applied Imagery Quick Terrain Modeler, and the University of North Carolina at Charlotte (UNC Charlotte) Light Detection and Ranging-based Bridge Evaluation (LiBE) surface damage detection algorithm were a few of the promising post-processing platforms under consideration. Currently, the majority of data refinement has been completed with TopoDOT. This was primarily due to the product's availability and prior understanding of the basic operating platform, Bentley MicroStation.

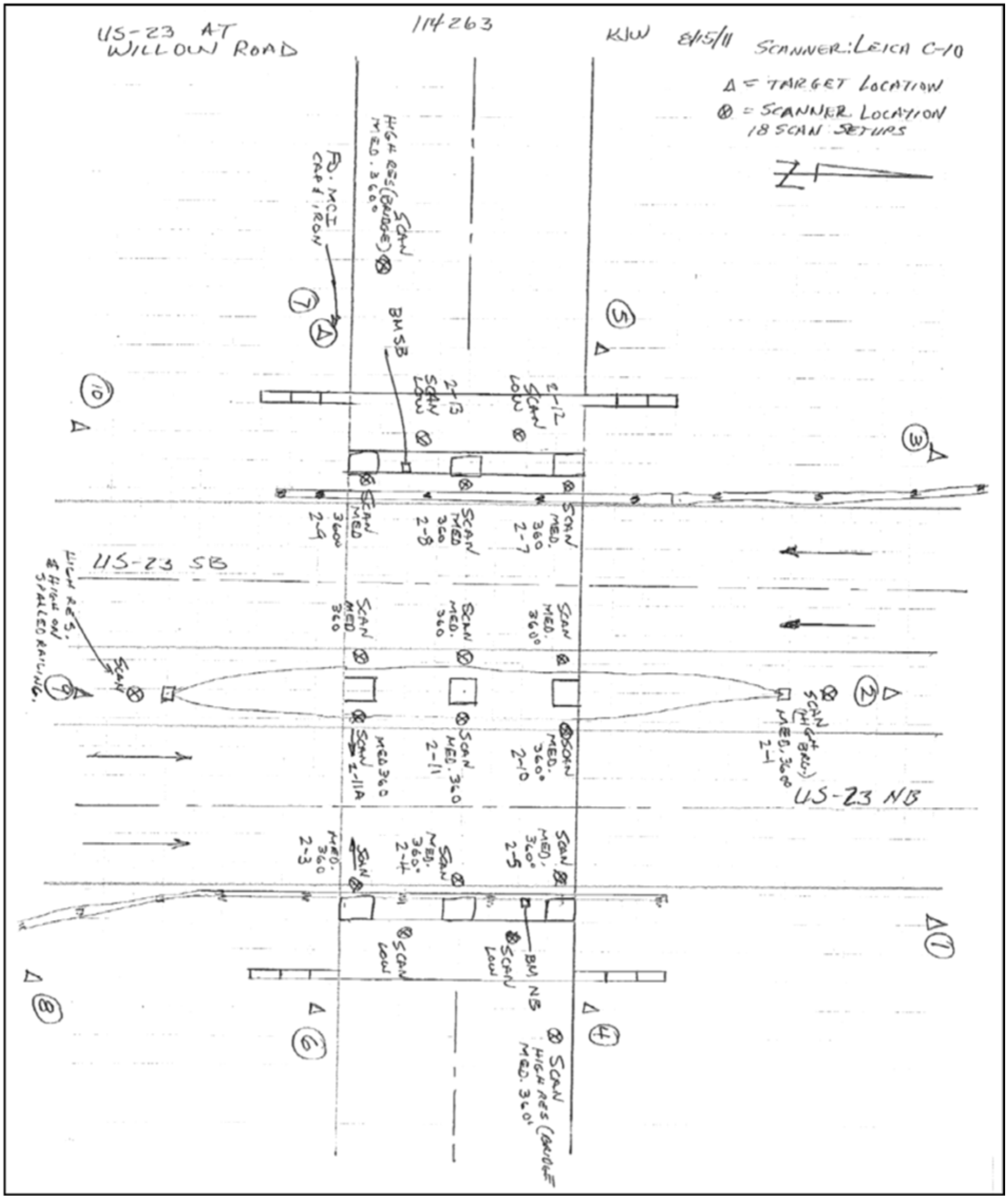

Figure 17: Field sketch for the LiDAR data collection made by the MDOT survey crew on the Willow Road bridge. The sketch documents the site configuration, scan locations, location of retro-reflectors and bench marks (used to register the individual scans to each other) and the resolution of the scans along with other information.

LiDAR data from setups at each site were merged together into a single registered and geo-referenced point cloud. The point cloud then was cropped to the area of interest (the bridge structures), reducing the file size and eliminating extra data. Attributes in the data include return intensity and elevation. MTRI staff has subset the data in order to analyze only the bridge deck surface and extract out condition information into separate LAS (Log ASCII Standard) files, such as the percent of the deck surface, underside, or support columns that are spalled.

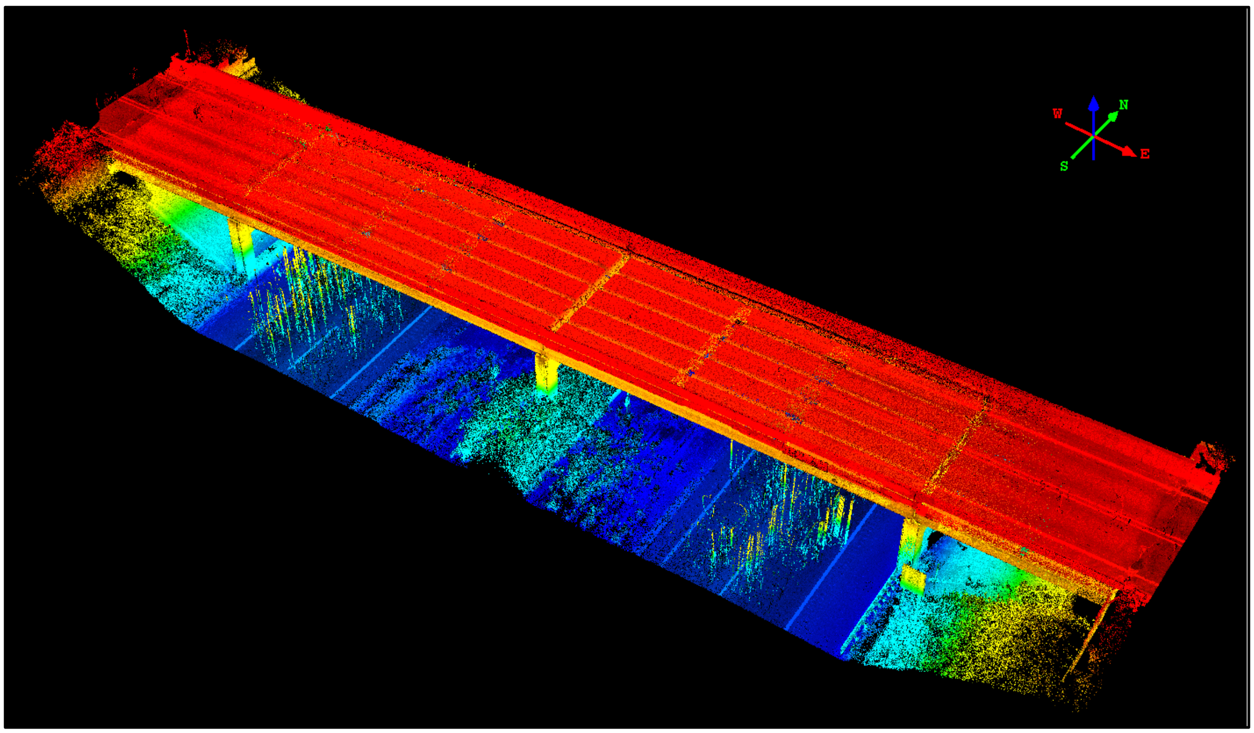

Figure 18: Registered, geo-referenced LiDAR point cloud of the Willow Road as collected by MDOT for this project. Point elevation (color) and intensity are displayed. This LiDAR point cloud contains more than 186 million points. The Willow Road bridge is approximately 209 ft long (63.7 m). Applied Imagery Quick Terrain Modeler software was used to generate the point clouds and DEMs.

Because the point clouds were so large, data collected at Willow Road bridge (and other sites) has been broken into subsets by bridge span to alleviate processing difficulties (see Figures 19, 20, and 21). Arch and crown in the bridge structure and deck may require sub-setting the data to separate the points on the bridge deck from the supporting structures. The quantity and location of the scanner setups can significantly affect the point density on the target surface. A point density image of the span of the Willow Road bridge over southbound US-23 shows the dramatic drop in point density with distance from the scanner, which was set up on the west approach of the bridge (see Figure 22).

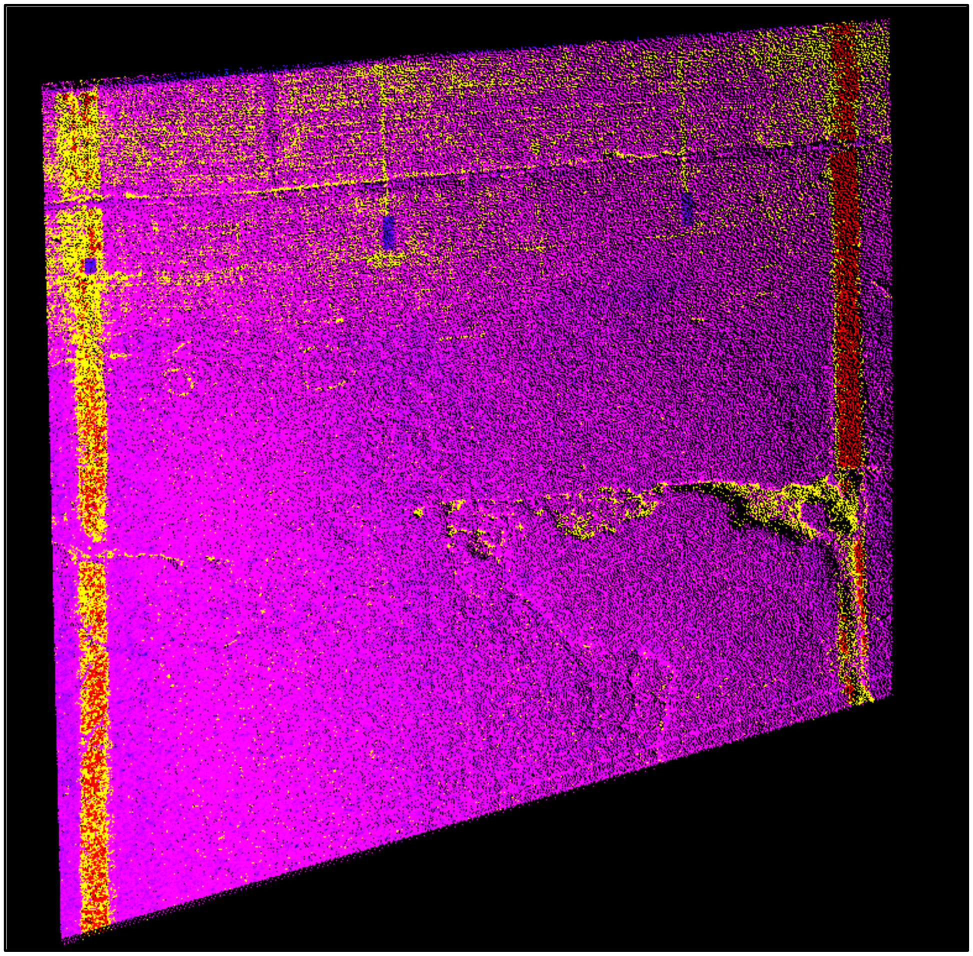

Figure 19: TopoDOT data of Willow Road bridge subset deck extraction, color intensity display.

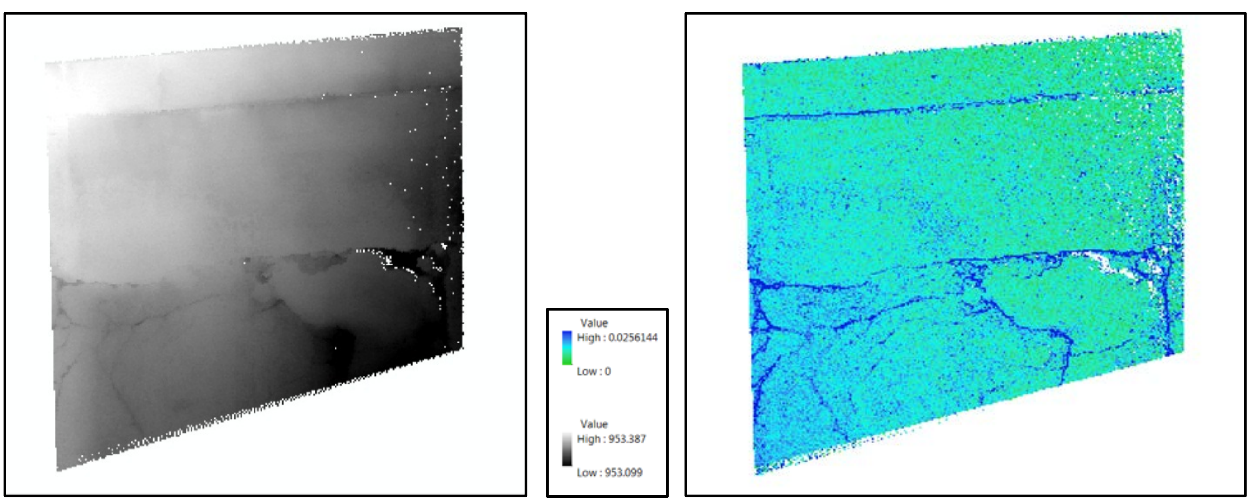

Figures 20 & 21: ArcGIS ArcMap Willow Road bridge subset deck DEM displaying point elevation (ft) and standard deviation from plane.

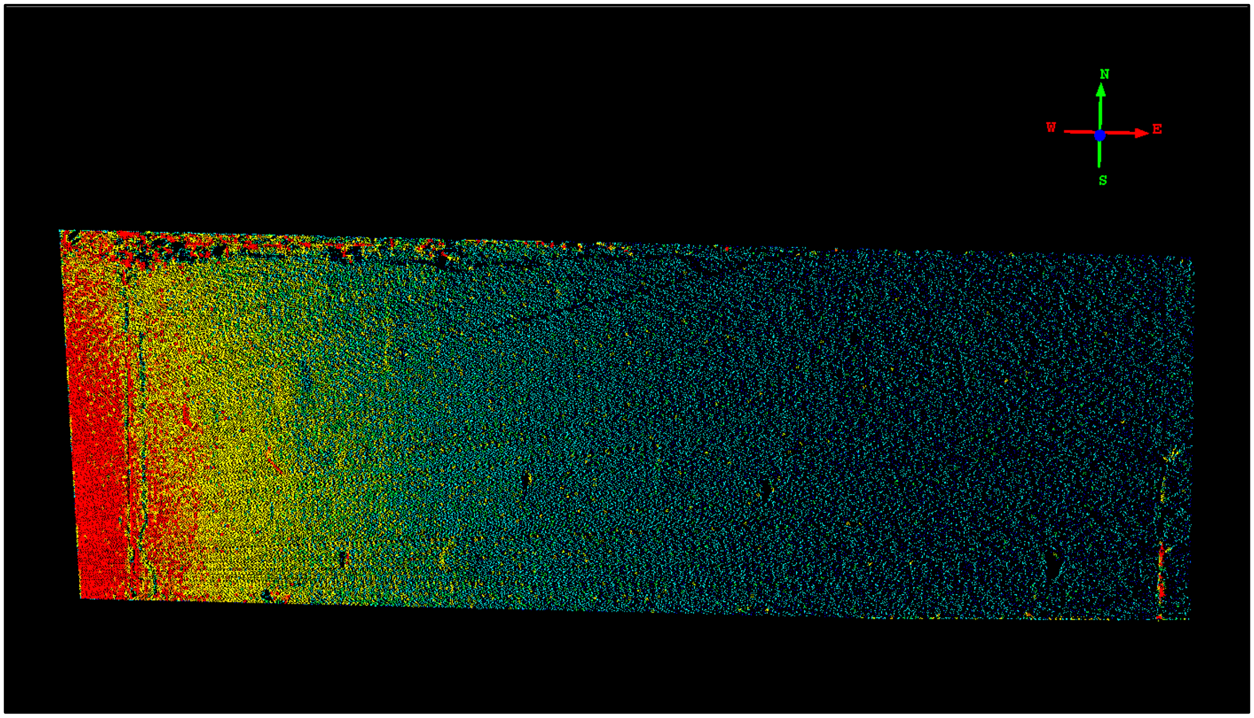

Figure 22: Point density image of Willow Road bridge span over southbound US-23. Note the dramatic fall-off in density of points from left to right (red to blue, high to low).

The color ramp is from red (high density) to blue (low density) which represents a range from approximately 25 points per 20 cm^2 (1.25 points/cm^2) grid cell to approximately 300 points per cell (15 points/cm^2). The distance between the LiDAR scanner and the left edge of this subset of the scan is approximately 50 ft (16.5 m). The scan resolution, slope of the surface to be scanned toward or away from the scanner and size of and distance to the features to be resolved are all important attributes to be considered when designing how many times and where the scanner is set up at a site. Potential shadowing and orientation of features to the scanner must be considered when placing the LiDAR scanner. Even small features can be affected by shadowing and scanner setup location should take that into account. Figure 22 is an example of the fall-off in point density as distance from the scanner increases. In this example, the scanner is approximately 51 ft from the left edge of the image. Features in the bridge deck that are closer to the scanner have a higher point density and can be more easily resolved than similar features further away from the scanner.

LiDAR returns usually include attributes such as RGB (red, green, and blue) and intensity (brightness) values in addition to X, Y, and Z location information. The MDOT LiDAR data processed here also contains 8 bit intensity information which is useful when interpreting the elevation data. Information about the relative reflectivity (intensity) of the bridge deck can be combined with color coded elevation data to provide clearer picture of the study area.

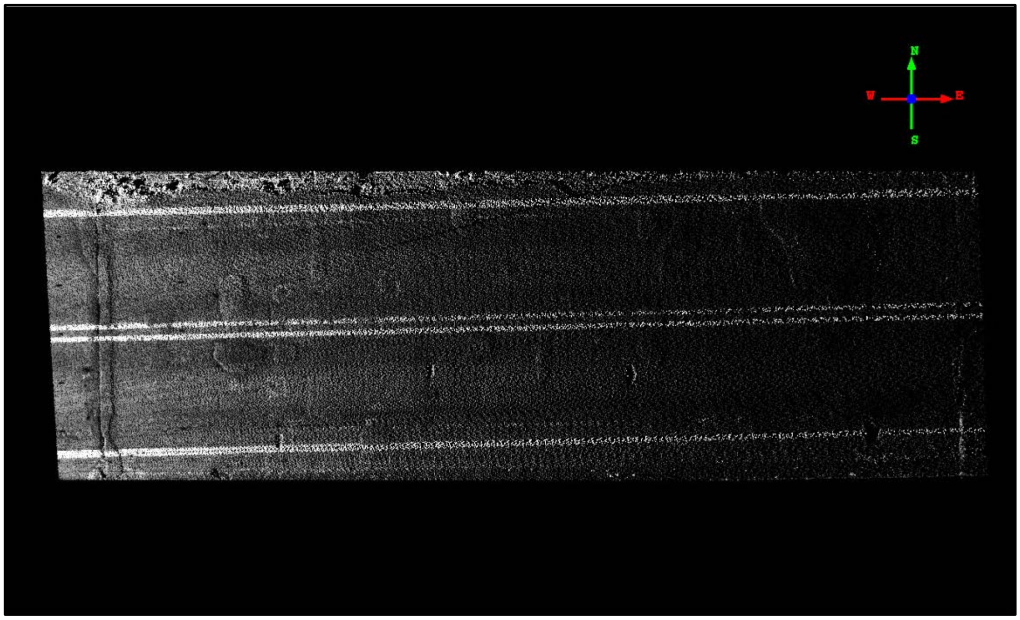

Figure 23: LiDAR intensity image of the Willow Road bridge span over southbound US-23.

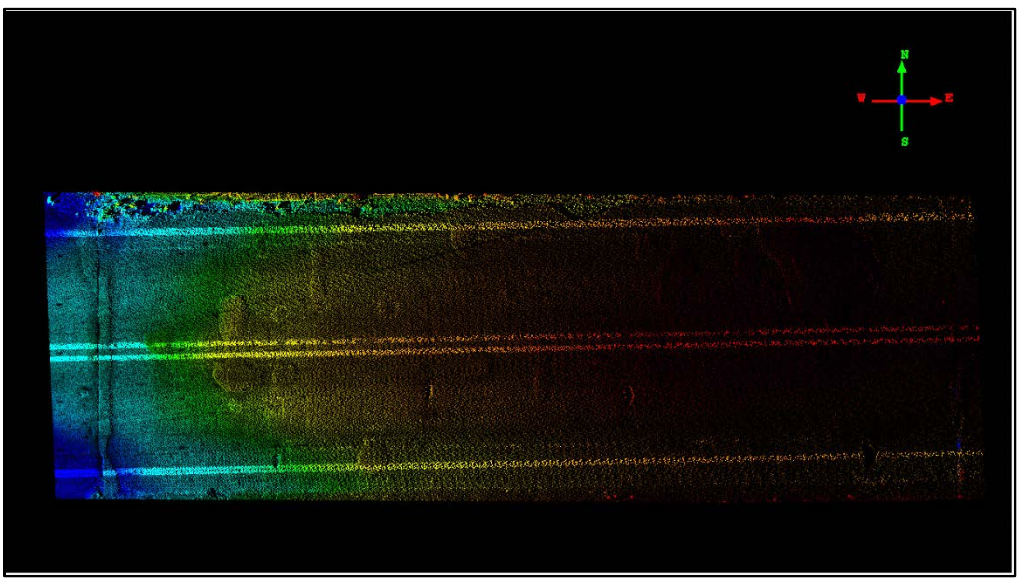

Figure 24: LiDAR intensity and elevation data displayed together provide a clearer picture of the condition of the bridge deck. This segment of the bridge deck is approximately 77 ft long. Total elevation change from left (low) to right (high) is 0.71 ft.

Deck specific information was then transferred into ArcGIS ArcMap, where the LAS file was converted to a working multipoint feature class, which allowed the user to build a terrain data set for the LiDAR points. From that working feature class the user was able to develop a DEM.

Currently, the DEM is being used as an input file for the spall detection algorithm. Figure 25 shows an example of highlighted defects (shown in red).

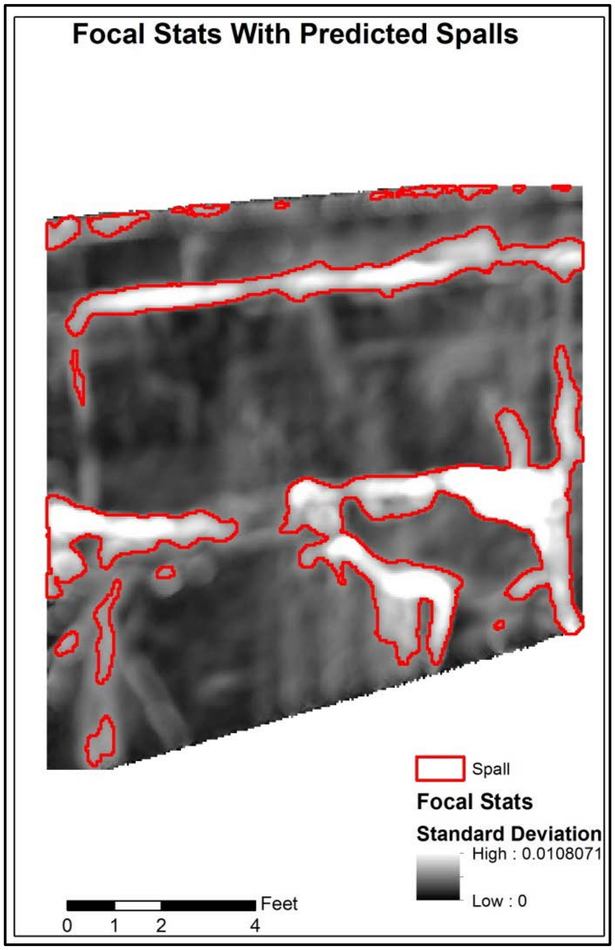

Figure 25: Willow Road subset deck focal statistic algorithm output highlighting predicted spall regions.

The DEM derived from the LiDAR data overlaid on ortho-photographs of the bridge is a useful technique to verify visual and quantitative analysis of the data. In this example a geo-referenced mosaic of bridge deck images captured by the 3DOBS system is used to help confirm the analysis of the deck condition seen in the LiDAR data. In Figures 26 and 27 patches made to the bridge deck that are not flush with the existing deck can be seen (arrows) as areas of slightly higher elevation. A spall can also be seen in Figures 26 and 27 as an area somewhat lower in height than the surrounding bridge deck. The patches are 0.25-to-0.625 in (0.635-to-1.59 cm) higher than the surrounding bridge deck and the spall at its deepest point is about 0.375 (0.953 cm) deep.

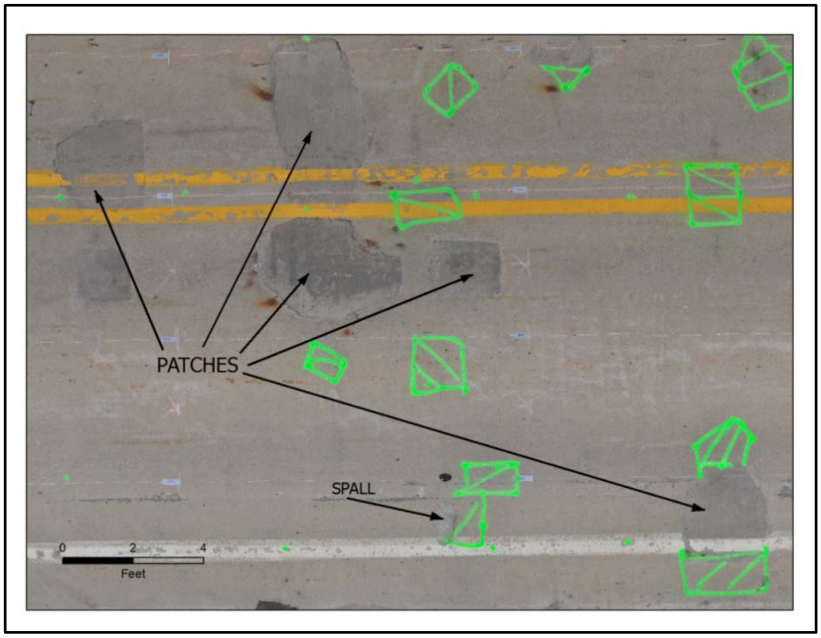

Figure 26: Section of the ortho-photo of the Willow Road bridge deck illustrating patches and a spall. The green pavement markings outline areas of subsurface delamination as determined by sounding performed by MDOT bridge inspectors with the hammer (rod) sounding technique.

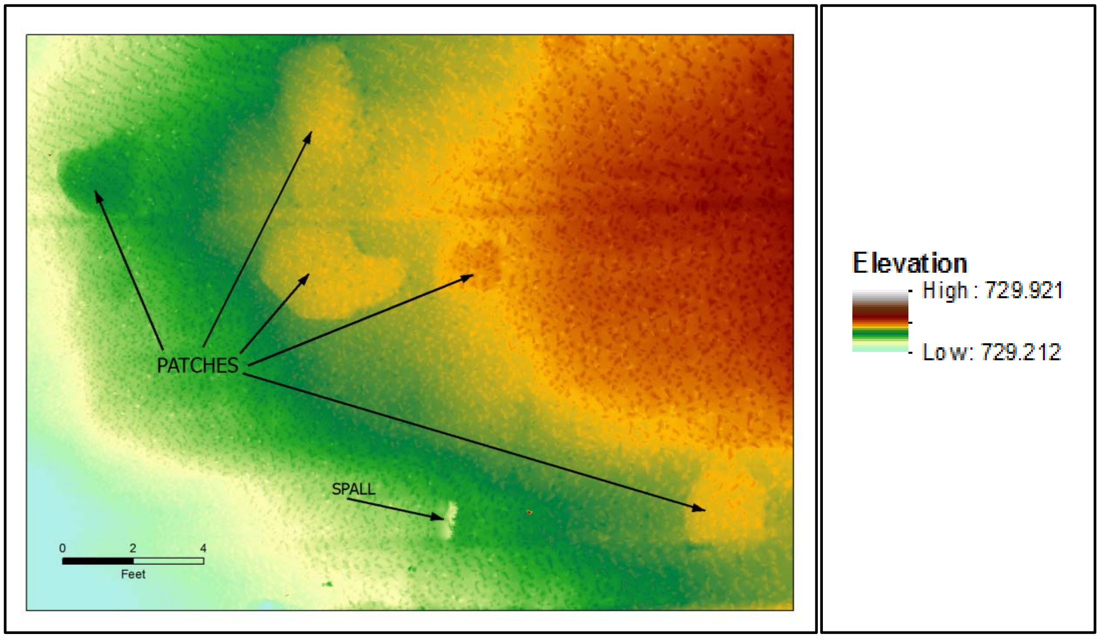

Figure 27: DEM with a color ramp applied of the same area of the Willow Road bridge deck. Note that the higher areas of the concrete patches and missing material from the spall correlate well between the ortho-photo and DEM. The patches (correctly) appear higher than the surrounding bridge deck and the spall appears lower than surrounding deck.

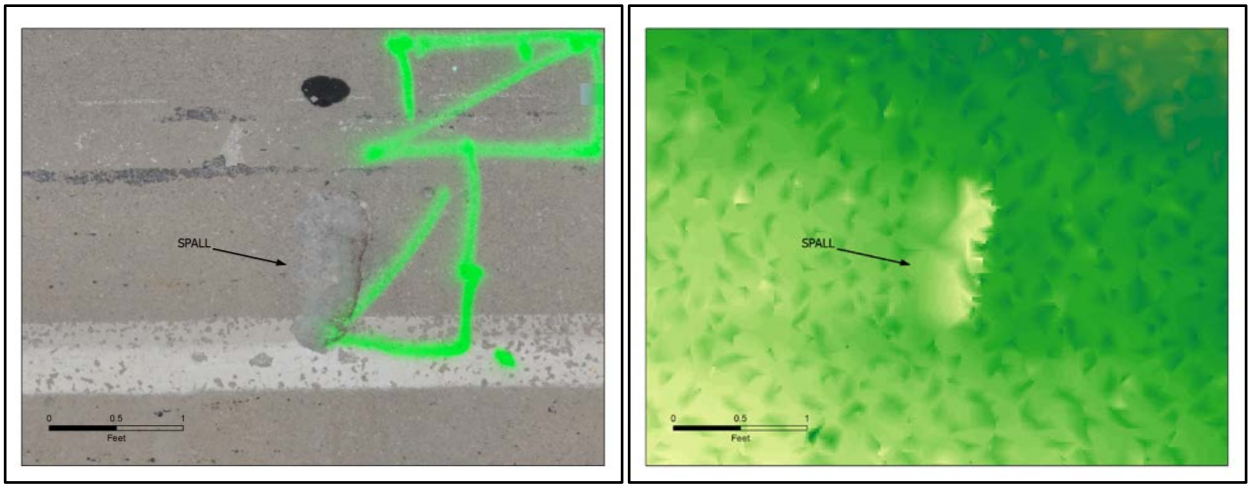

Figure 28: Close up of the spall on the Willow Road bridge deck. The spall is clearly visible in the ortho-photo as well as in the DEM (the light yellow color is lower than the green).

Next Steps

For LiDAR data processing, the next step is to take the DEMs of sections of the bridge deck that have been exported and process them in the 3DOBS spall detection algorithm. Adjustments to the DEMs will be made based on the results of the processing until the best possible result is obtained during the next quarter.

As it has been mentioned in technical memorandums nº 20 and nº 21, LiDAR is a line of sight instrument and requires repositioning to illuminate shadowed areas, increasing collection time and required labor. The line-of-sight issue meant for the terrestrial LiDAR system used by MDOT, areas further away from the collection point were characterized with fewer points. A mobile LiDAR system could address such an issue, although mobile LiDAR systems generally have lower overall accuracy capabilities than fixed terrestrial LiDAR systems, at least compared to areas near the fixed LiDAR system itself. Mobile LiDAR has the potential to reduce the collection time and increase the resolution as discussed in technical memorandum nº 21. Surveying Solutions (<http://www.ssi-mi.com/>) has scanned the I-96 and US-23 interchange in southeast Michigan using mobile LiDAR and MTRI is in the process of acquiring that dataset. The resolution and coverage of the dataset is unknown at this time; however, once acquired, the data will be assessed in a similar manner to the terrestrial LiDAR for its potential as a tool for bridge condition assessment.

As results of processing of DEMs are evaluated, a recommended LiDAR data collection and processing workflow will be developed to create the final condition metric, which is anticipated to be at least the percent spalled area of the bridge deck surfaces. Because the terrestrial LiDAR system can be positioned almost anywhere near or under a bridge (which was demonstrated during MDOT's data collection), it may be possible to characterize the number and volume of spalls in other parts of the bridge infrastructure as well, such as bridge piers and the deck underside. This is being investigated in the next quarter.

The high-resolution elevation profile created through the 3DOBS is an alternative to intensive LiDAR data collection and analysis process; it creates consistent, high resolution data across the entire deck surface without the need for a mobile or fixed LiDAR system. An evaluation (both technical and economic) of LiDAR elevation data versus the 3DOBS elevation data in creating useful bridge condition data is expected to be a very useful outcome of this project.

ULTRA WIDE BAND IMAGING RADAR SYSTEM (UWBIRS)

Most commercially available ground penetrating radar (GPR) systems for bridge deck assessment use arrays of antennas pointed perpendicular to the deck to probe the subsurface. As noted in the Commercial Sensor Evaluation report (<http://www.mtri.org/bridgecondition/doc/RITA_BCRS_Commercial_Sensor_Evaluation.pdf>), these systems can sense subsurface defects, but can require substantial time to survey the deck. These commercial systems can provide output products for use in the DSS, such as the location of delaminations. To potentially improve data collection efficiency, the current project has been investigating the idea of using side-looking, low cost ultra wide band imaging GPR, now referred to as UWBIRS. This type of collection is consistent with a concept of operation that has a radar system mounted on a moving vehicle to produce maps of deck radar reflectivity that identify areas of concern. This type of collection could also be performed by a standoff airborne sensor. An issue with this approach is whether or not the subsurface deck defects will be uniquely indicated when the deck is illuminated obliquely by the radar.

Side-looking imaging GPR measurements of concrete bridge decks were conducted in August, 2011 as part of the field demonstrations. Specifically, data were collected at the Freer Road bridge and the Willow Road bridge. The field measurements and radar equipment were recently well summarized in technical memorandum nº 21. In the 2D imaging modality, the radar sensor obliquely illuminated the bridge deck surface as it was moved along a linear path parallel to the deck surface. This type of data collect produces a 2D map of the radar reflectivity of the deck, which may indicate areas of internal defect and/or delamination. The deck measurements at the Freer Road bridge were repeated on December, 2011 to fill in some missing data areas from the earlier August, 2011 collect.

The primary activity during the reporting period was to processed the collected radar data into radar images, geo-reference the images so that they could be displayed with other sensor products in the DSS, and finally compare the images to polygon overlays that indicate potential delamination areas, which were identified by MDOT using the hammer sounding technique during the August, 2011 data collection. Images of the two lanes of the Willow Road bridge deck when calibration reflectors were placed in the scene are shown in Figure 29 with potential delamination sites from the ground truth survey overlaid. It is these types of analyzed radar results that the project team has been planning to integrate into the DSS to show where radar has detected these likely delamination results, as well as the locations and percent of delamination. These data would contribute to the overall bridge health signature being developed for this project.

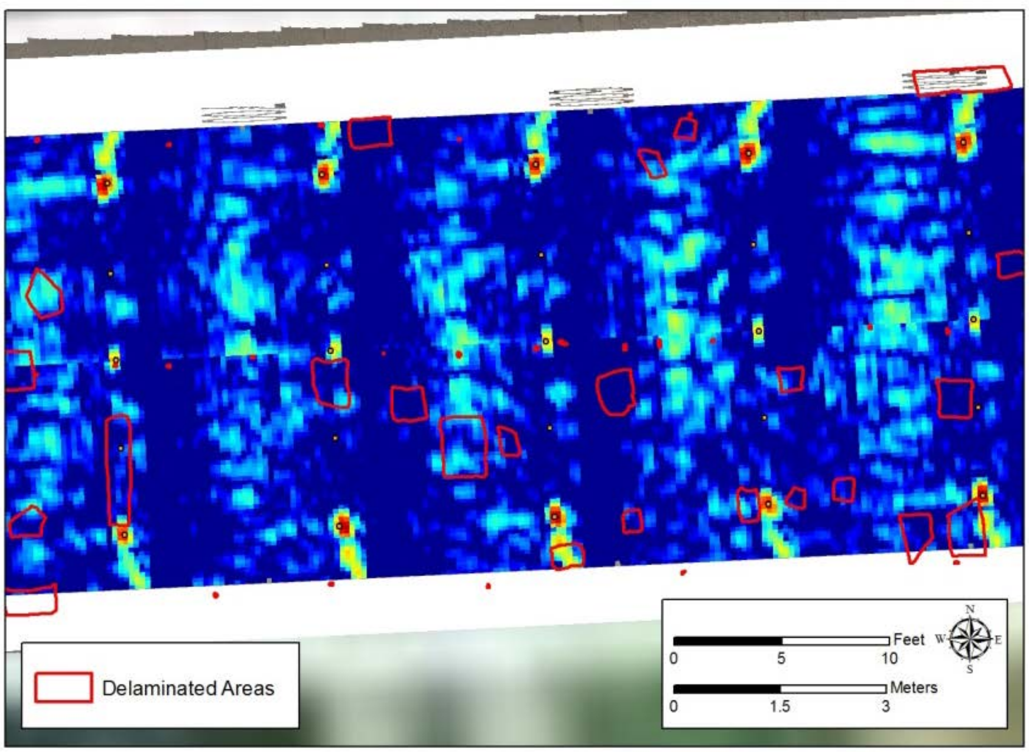

Figure 29: Radar image of Willow Road bridge deck with delamination areas indicated by red polygons.

Next Steps

Even though the side looking GPR images show variation that is likely due to variation in the bridge structure, an initial qualitative comparison of the side looking GPR images with the delamination ground truth suggests that the high return areas in the radar images do not uniquely identify the delamination areas. This preliminary result suggests that a limitation of obliquely illuminating the bridge deck is that near surface delaminations cannot be uniquely separated from other variations in the bridge substructure. The next step in the analysis will be to quantitatively compare the variations in the radar images to the ground truth information in order to evaluate the utility of the radar data and system for deck assessment. The team also plans to investigate the use of alternate imaging parameters and/or post-processing to enhance measurement performance.

UWBGPR data from conventional commercially available systems can provide delamination information for use in the DSS, albeit at the cost of more data collection time, even if the side-looking concept investigated through this project does not prove viable. The Commercial Sensor Evaluation noted the HERMES system (Scott et al. 2001 at <http://www.fhwa.dot.gov/publications/research/nde/pdfs/01090.pdf> and <https://www.llnl.gov/str/Hernandez.html>), described as the "bridge diagnosis at 55 mph" system focused on delamination detection.

A related system is the Roadscanners commercial GPR data analysis system, which characterizes bridge decks including areas of subsurface deterioration (see <http://www.roadscanners.com/uploads/PDF/Bridge_web.pdf>). Based on these descriptions the Roadscanners system and of HERMES and its successor, the PERES Bridge Inspector (<http://ntl.bts.gov/DOCS/peres.htm >), the project team anticipates that data from such a system could provide the needed delamination data for inclusion in the DSS. As a next step, the project team is pursuing contacts with the HERMES/PERES team at FHWA and Lawrence Livermore National Lab and Roadscanners to see if a representative delamination data set could be shared to serve as a firm example of the type of result that could be included in the DSS.

ADDITIONAL TECHNOLOGIES UNDER EVALUATION

During the past quarter, major additional work was not pursued for the "additional technologies" of using Synthetic Aperture Radar (SAR) for evaluating the inside of concrete box beams, using Interferometric Synthetic Aperture Radar (InSAR) for bridge deck settlement, using InSAR data for deck condition, and using Multispectral Satellite Imagery (MSI) for bridge deck condition evaluation.

Instead, the team focused on the main technologies such as the 3DOBS, ThIR, DIC, LiDAR, and the UWBIRS. The project team expects to conclude and write up these additional technology investigations during the next quarter.

DECISION SUPPORT SYSTEM (DSS)

Since the last quarterly report, a number of improvements have been made to the DSS and development is ready to focus on the last major feature, the integration of remote sensing data, before testing and mobile app versioning. These include refactoring the server-side data models based on the Pontis schema, importing data from MDOT's Transportation Management System (TMS), and the utilization of new bridge information derived from remote sensing in the DSS through new features.

Migration to the Pontis Database Schema

A few months ago, the DSS team gained direct read access to MDOT's TMS database, an Oracle database based, in part, on the Pontis schema. When DSS development began in March, 2011, MTRI only had partial database exports shared by MDOT to use in designing the server and database schema. As a result, the schema that was developed and much of the client-side architecture were based on a data model that MDOT bridge managers and inspectors were used to working with. This data model was also amenable to visualization in a Geographic Information System (GIS), a planned feature for the DSS.

The DSS team members have since decided, however, that this data model, while amenable to geo-spatial visualization, is not as flexible, extensible and informative to end users as it ought to be. In particular, this data model could not answer questions such as "*How does, for instance, the Texas Department of Transportation load their bridge data into the DSS?*" and, more generally, "*How would transportation agencies in other states make sense of bridge data in the DSS?*" Furthermore, this data model limited attempts to update the DSS with new bridge condition information. The DSS team had intended to accomplish this through regular data exports from TMS. However, without the queries used by MDOT employees to generate the tables the DSS team had based our data model on, it was not practical to export usable data from the TMS. Consequently, the DSS would go without updates.

As being able to have frequently updated bridge condition information is important even for a demonstration tool, the DSS team decided a data model consistent with the TMS was needed. Within Pontis, the National Bridge Inspection System (NBIS) lays out a national standard for storing bridge inspection data and bridge metadata. The TMS database uses this standard for its relevant bridge tables. To facilitate quick DSS updates from the TMS database, the DSS team decided to modify its initial data models to match that of the bridge tables in the TMS.

There are always challenges to redesigning a database schema, particularly relatively late in the life of a software project using a database application programming interface (API). Many technical challenges arose simply because the DSS and the full TMS database use different database management systems (DBMS); the DSS is based on a flexible, open source PostgreSQL database while TMS uses an Oracle database. The most fundamental obstacle this posed was that it prevented the DSS from reading the TMS database directly: data would have to be exported form the TMS and inserted into our database. Different DBMSs led to irreconcilable differences between the TMS database schema and what would eventually be used in the DSS, such as the lack of a distinction between *null* and *blank* fields in Oracle, differing data types, and the implication of foreign keys in the TMS database that are never actually used. Overall, these differences are relatively trivial obstacles. However, the most serious and persistent obstacle for development of effective data models of bridge condition was the mismatch between the representation of data in the application (front-end) and service (back-end) layers. This mismatch is often referred to as *object-relational impedance mismatch* because it arises when object-oriented frameworks, such as the Ext JS framework used to develop the client-side web application and the Python language used to support server programming, are used in conjunction with relational databases.

The DSS was designed to represent the latest condition information for multiple bridges at a time using bridge attributes such as facility carried, latitude, and longitude. In the TMS, under the Pontis schema, condition information and bridge attributes are stored in different tables which are not related. This requires the developer to make a decision about how the DSS will access the information stored in both tables quickly (whenever users make a query) and comprehensively. The DSS team realized there were only two practical solutions: run the "*What's the latest condition of each bridge?*" query in real time, every time, or create an intermediate table to store this query. The former would be slow and expensive but the latter would store redundant data in the database. The DSS team decided to create an intermediate table because its contents would need to be accessed too frequently to justify the expensive calculations involved in a *virtual table* created from querying the database in real time.

New Bridge Attributes and the Value Added

Despite the aforementioned obstacles, migrating to the Pontis schema enables new, meaningful and up-to-date bridge attributes to be exposed through the DSS, and leads to a system that could be used across multiple states for bridge condition assessment. In the original small MDOT bridge data export, even simple attributes like the county a bridge is located in were not available (since it was not part of the data exports given to us) before data from TMS were integrated. These new attributes led to the development of a new feature: attribute tables for each bridge (Figure 30). These tables correspond to the new tables available from Pontis. While most of the information they contain is unnecessary or inappropriate to display in the metrics table to the left, it is still extremely valuable and of interest to the bridge manager or inspector. Accessing these data through an *attribute table* is a workflow borrowed from GIS that seems very appropriate when the user is capable of visualizing up to 12,000 bridges.

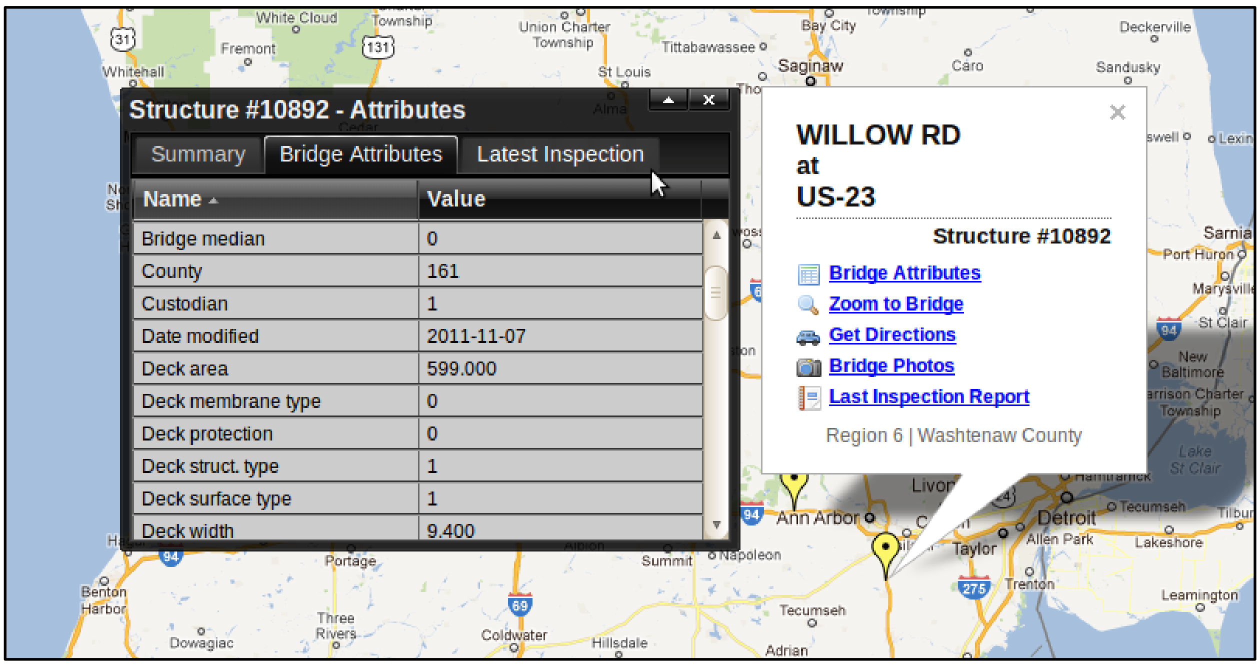

Figure 30: Migrating to the Pontis schema has made new data available; though in separate tables, they can be accessed individually through the "Bridge Attributes" utility.

In addition to the "Bridge Attributes" table, a link to the "Bridge Photos" utility is also now available through the DSS' Bridge GIS plane. The "Bridge Photos" utility displays location-tagged photographs of the bridge deck, approach and underside that were taken with the BVRCS. These photos are displayed both as thumbnails and a points layer in Bridge GIS showing the position from which they were taken (Figure 31). A full-resolution version of the geo-referenced photos is available through both.

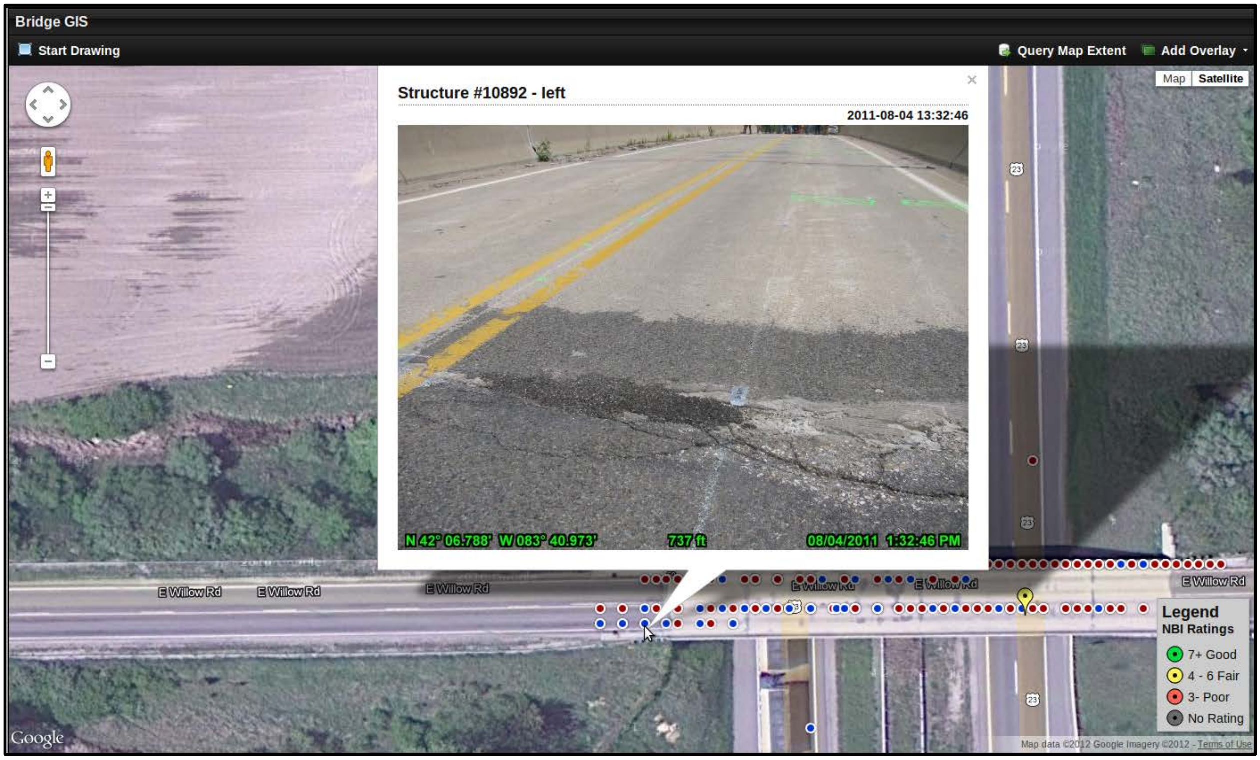

Figure 31: Geo-tagged photographs from the BVRCS are available as a Points layer in Bridge GIS; clicking on a point shows you the photograph taken there.

Integrating Data and Deriving the Bridge Condition Signature

The next major phase of the DSS development has begun with the integration of the remote sensing data like the BVRCS photographs. These photos are an example of a "points" layer representation of remote sensing inputs for bridge condition. Other examples can be seen in the concept diagram, Figure 32, including examples of "polygon" datasets (such as areas of spalls collected by the 3DOBS) and extremely high-resolution georeferenced composite images of the deck surfaces (also created through the 3DOBS). This refers to how these datasets will be represented in the DSS. The more important question, however, is how will these datasets be integrated with each other and important metrics of bridge condition derived from them?

The summary data (Figure 32) the project team can now expect to derive from bridge remote sensing data include the percent spalled, the percent delaminated, the roughness (as an IRI score), and potentially crack density and count. Deflection amount and settlement may be possible to integrate depending on final remote sensing results. These should be related to NBI condition indicators wherever possible, such as the amount of spalling that results in a certain NBI rating. These will be integrated in what has been referred to from the project's beginning as the bridge condition *signature*. An example formula to derive such a notion for a bridge deck surface rating (BDSR) is given below, where “a, b, c, and d” are user-defined weights:

$$\text{BDSR} = a \times [\%\ \text{spalled}] + b \times [\%\ \text{delamination}] + c \times [\text{roughness index}] + d \times [\text{crack density}]$$

Next Steps

With the remote sensing technologies producing results such as percent spalled, percent delaminated, and bridge deck roughness, the project has reached the intended stage of integration-usable indicators of bridge condition into a decision support system. This is a critical step to having an overall bridge condition assessment system (technologies plus the DSS) that is practical to use by transportation agencies. The next Quarterly Report will update the team's progress on reaching this important project milestone.

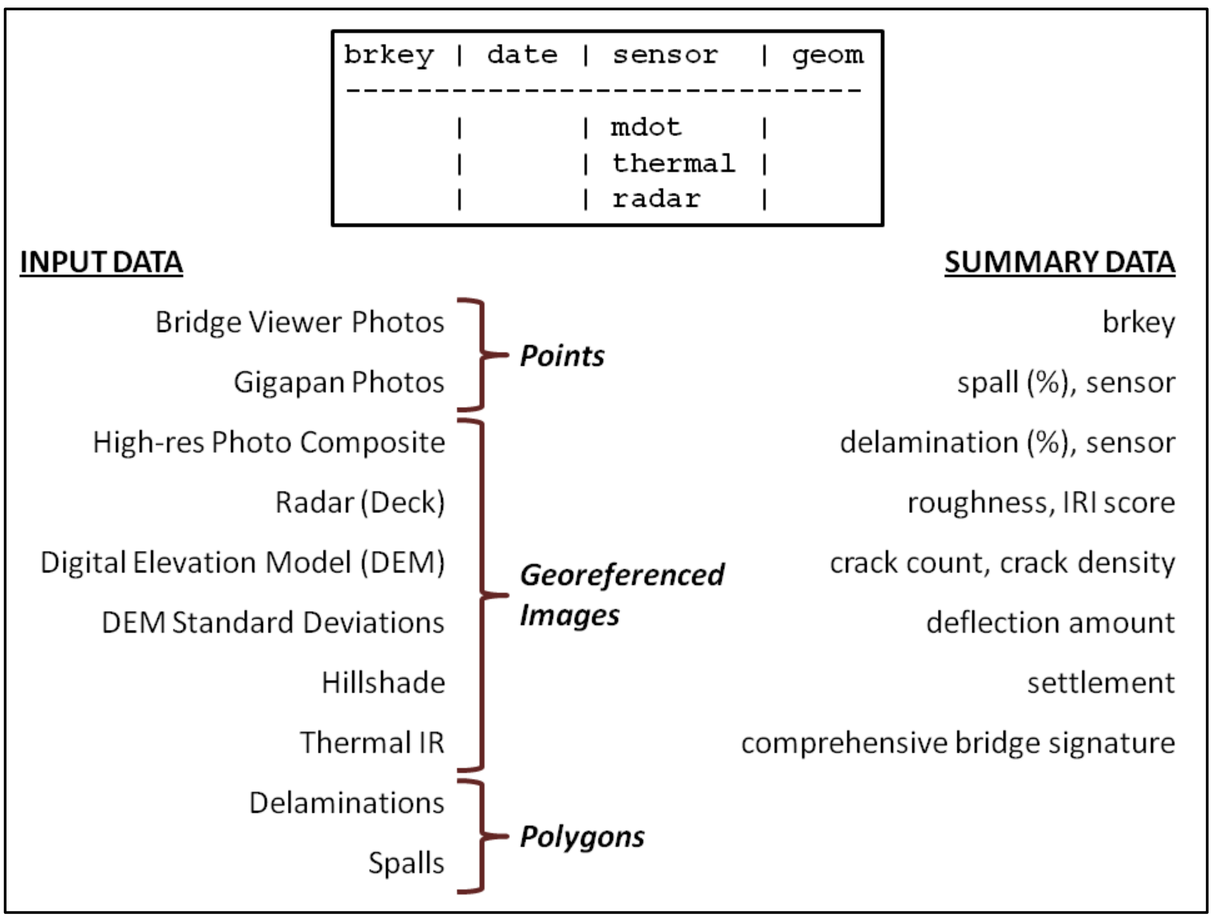

Figure 32: Concept diagram for remote sensing datasets and their role in the DSS.

REFERENCES

Scott, Michael, Ali Rezaizadeh, Mark Moore. 2001. Phenomenology Study of HERMES Ground Penetrating Radar Technology for Detection and Identification of Common Bridge Deck Features. FHWA Report No. FHWA-RD-01-090, Turner-Fairbank Highway Research Center, 33 pgs. Retrieved at <http://www.fhwa.dot.gov/publications/research/nde/pdfs/01090.pdf>.